Herzberg circuit and Berry's phase in chirality-based coded qubit in a triangular triple quantum dot

Chang-Yu Hsieh, Alexandre Rene, and Pawel Hawrylak

Quantum Theory Group, Institute for Microstructural Sciences, National Research Council, Ottawa, Ontario, Canada K1A 0R6 and Department of Physics, University of Ottawa, Ottawa, Ontario, Canada K1N 6N5

(Received 18 October 2011; revised manuscript received 8 May 2012; published 6 September 2012)

We present a theoretical proposal for the Herzberg circuit and controlled accumulation of Berry's phase in a chirality-based coded qubit in a triangular triple quantum dot molecule with one electron each. The qubit is encoded in the two degenerate states of a three-spin complex with total spin $S = 1/2$. Using a Hubbard and Heisenberg model the Herzberg circuit encircling the degeneracy point is realized by adiabatically tuning the successive on-site energies of quantum dots and tunnel couplings across a pair of neighboring dots. It is explicitly shown that encircling the degeneracy point leads to the accumulation of the geometrical Berry's phase. We show that only the triangular, not the linear, quantum dot molecule allows for the generation of Berry's phase and we discuss a protocol to detect this geometrical phase.

DOI: 10.1103/PhysRevB.86.115312 PACS number(s): 81.07.Ta, 03.65.Vf, 73.21.La

I. INTRODUCTION

As discussed by Herzberg[1] and Berry,[2] the wave function acquires a geometric phase,[3] Berry's phase, when it is adiabatically moved along a circuit in the parameter space of the Hamiltonian, the Herzberg circuit, enclosing a degeneracy point. Since only the topology (enclosing a degeneracy point or not) of the Herzberg circuit determines whether the geometrical phase is accumulated, the Berry's phase is less sensitive to the effects of interactions between the system and its environment. For this reason there is interest in attempting to encode and manipulate quantum information in geometric phases, for example holonomic quantum computing[4] with a generalized non-Abelian geometric phase.[5]

Experimentally, Berry's phase in two-level systems has already been demonstrated, including neutron[6] and nuclear spins,[7] superconducting qubits,[8] and a superconducting charge pump.[9] Preceding the successful experiments with superconducting circuits, the relation between Berry's phase of a superconducting circuit and other measurable quantities was investigated theoretically,[10,11] including a theoretical proposal for realizing geometric quantum computation with superconducting qubits.[12]

In this work, we demonstrate theoretically the generation of the Herzberg circuit and Berry's phase in quantum states of a three-electron complex in a half-filled triangular triple quantum dot molecule in a field-effect transistor within the framework of Hubbard and Heisenberg models. The two-level system, a qubit, is encoded in the two degenerate states of a three-spin complex with total spin $S = 1/2$.[13–15] An early proposal to generate the geometrical phase in degenerate one-electron quantum levels of a three-atom system was discussed by Herzberg and Longuet-Higgins in Ref. 1 in 1963. A triple quantum dot (TQD) molecule studied here is related to the three-atom system. We define a two-level system, coded qubit,[13,14] by the two lowest degenerate levels of a half-filled three-electron TQD under an in-plane magnetic field. It was shown that the quantum states of a coded qubit in a TQD can be manipulated by tuning the gate voltages.[13,14] This opens the possibility described in this work to engineer the Hamiltonian to undergo adiabatic and cyclic evolution along the Herzberg circuit resulting in accumulation of Berry's phase. Recent experiments[16–19] on the linear TQD have already demonstrated the high tunability and coherent manipulation of the many-body quantum states in a TQD. However, we show that it is not possible to generate a Herzberg circuit for a linear triple quantum dot, only for a triangular triple quantum dot molecule with control over quantum dot energies and at least one tunneling amplitude.

The plan of the paper is as follows. In Sec. II, we describe the system and the Hamiltonians for a triangular and linear TQD. In Sec. III, we construct a Herzberg circuit generating Berry's phase in a triangular TQD. We show that it is not possible to construct the Herzberg circuit for a linear TQD. In Sec. V, a brief conclusion is given.

II. THE MODEL

A lateral TQD is defined by metallic gates on top of a two-dimensional electron gas in the (x,y) plane at the GaAs/AlGaAs heterojunction with three local minima, capable of confining a controlled number of electrons. With one electron in each dot, the extended Hubbard Hamiltonian reads

$$\hat{H}_{\text{hubb}} = \sum_{i=1}^{3} E_i \hat{n}_{i\sigma} + \sum_{\substack{i,j=1 \\ i\neq j}}^{3} \sum_{\sigma} t_{ij}(\mathbf{B}) \hat{c}^{\dagger}_{i\sigma} \hat{c}_{j\sigma} + \frac{1}{2} \sum_{\substack{i,j=1 \\ i\neq j}}^{3} V_{ij} \hat{\rho}_i \hat{\rho}_j + \sum_{i=1}^{3} U_i \hat{n}_{i\uparrow} \hat{n}_{j\downarrow} + \sum_{\alpha} g \mu_B \mathbf{S}_{\alpha} \cdot \mathbf{B}, \tag{1}$$

where $\hat{\rho}_i = \hat{n}_{i\uparrow} + \hat{n}_{i\downarrow}$, E_i is the on-site energy, and t_{ij} is the tunnel coupling between dot i and dot j which acquires the Peierl's phase if field $\mathbf{B}$ is applied perpendicular to the closed-loop structure of a triangular TQD. V_{ij} is the long-range Coulomb interaction between dot i and j, U_i is the on-site Coulomb interaction of dot i, g is the g factor of the host semiconductor, μ_B is the Bohr magneton, and $\mathbf{S}_{\alpha}$ is the spin of the αth electron. For the present study, we set $t_{ij} = t = -0.05$ Ry*, $E_i = 0$, $U_i = U = 2.0$ Ry*, and $V_{ij} = V = 0.5$ Ry* as the initial state of the isolated triangular

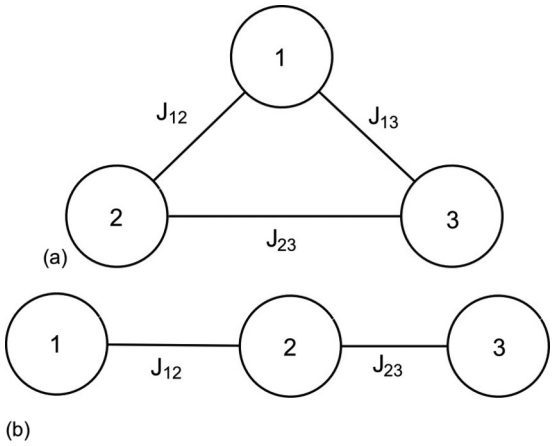

FIG. 1. (a) Schematic representation of a triangular triple quantum dot. (b) Schematic representation of a linear triple quantum dot.

TQD system. $\mathrm{Ry}^* = 5.97$ meV is the effective rydberg in GaAs. For the linear TQD case, we set $t_{13} = 0$ and $V_{13} = V/2$. In this analysis, we assume E_i and t_{ij} are independently tunable parameters that will be varied to generate Berry's phase. Figures 1(a) and 1(b) show the schematic picture of a triangular and a linear TQD, respectively.

As discussed in Ref. 20, the two arrangements of a TQD lead to two topologically different Hamiltonians. The low-energy spectrum (4 spin-3/2 and 4 spin-1/2 states) of a half-filled TQD is mapped onto the Heisenberg model[14,21,22] with one localized spin in each dot,

$$H = \sum_{i<j} J_{ij}\mathbf{S}_i \cdot \mathbf{S}_j + \sum_i g\mu_B \mathbf{S}_i \cdot \mathbf{B} + \sum_{i<j<k} \chi_{ijk}\mathbf{S}_i \cdot (\mathbf{S}_j \times \mathbf{S}_k), \quad (2)$$

where the exchange interactions J_{ij} can be derived from the Hubbard model and expressed by microscopic parameters as

$$J_{ij} = 2|t_{ij}|^2\left(\frac{1}{U - V + (E_i - E_j)} + \frac{1}{U - V - (E_i - E_j)}\right). \quad (3)$$

The coefficient χ_{ijk} for the chirality operator in Eq. (2) is nonzero only for a triangular TQD in the presence of a perpendicular magnetic field and is much smaller than J_{ij}.

Since the Heisenberg Hamiltonian commutes with the total S_y operator of the system, we focus on the $S_y = -1/2$ subspace. We further assume that an in-plane magnetic field B_y has been applied to separate the $S_y = -1/2$ and $S_y = 1/2$ subspaces by the Zeeman energy. In the $S_y = -1/2$ subspace, a resonant triangular TQD with all $J_{ij} = J_0$ has the following three eigenstates:[13,14,20]

$$|q_s\rangle = \frac{1}{\sqrt{3}}(|\downarrow\downarrow\uparrow\rangle + e^{i(2\pi s/3)}\,|\downarrow\uparrow\downarrow\rangle + e^{i(4\pi s/3)}\,|\uparrow\downarrow\downarrow\rangle), \quad (4)$$

where $s = 0, \pm 1$ and spin configurations, such as $|\downarrow\downarrow\uparrow\rangle$, label the electron spins in quantum dots from spin up in dot 1 (rightmost) to spin down in dot 3 (leftmost). The two chiral states, $|q_+\rangle \equiv |q_{+1}\rangle$ and $|q_-\rangle \equiv |q_{-1}\rangle$, constitute the two levels of a chirality-based coded qubit in a triangular TQD. The coherent manipulation of a coded qubit is achieved by tuning the exchange interactions J_{ij}. In the basis of the $\{|q_\pm\rangle\}$, the Heisenberg Hamiltonian reads

$$H_{\mathrm{tri}}^{\mathrm{qb}} = \frac{1}{4}(2J_{23} - J_{13} - J_{12})\hat{\sigma}_x + \frac{\sqrt{3}}{4}(J_{13} - J_{12})\hat{\sigma}_y, \quad (5)$$

where $\hat{\sigma}_i$ is the Pauli matrix with $i = x, y$. Equation (5) shows that a chirality-based coded qubit is equivalent to spin-1/2 under an effective magnetic field in the X-Y plane.

For the fully resonant, half-filled triangular TQD, the two degenerate states of the chirality-based coded qubit can be also rotated to the Jacobi states, $|L_0\rangle = \frac{1}{\sqrt{2}}(|\downarrow\downarrow\uparrow\rangle - |\uparrow\downarrow\downarrow\rangle)$ and $|L_1\rangle = \frac{1}{\sqrt{6}}(|\downarrow\downarrow\uparrow\rangle - 2|\downarrow\uparrow\downarrow\rangle + |\uparrow\downarrow\downarrow\rangle)$. The two sets of states $|q_\pm\rangle$ and $|L_{0,1}\rangle$ are related through linear transformation given in Ref. 14. The two Jacobi states $|L_0\rangle$ and $|L_1\rangle$ may be physically distinguished by the joint spin states on dot 1 and dot 3. The spins in dot 1 and dot 3 form a spin singlet in the state $|L_0\rangle$ while they form a linear combination of spin triplets with projections $S_y = -1$ and $S_y = 0$ in $|L_1\rangle$. The measurement of the joint spin states (singlet versus triplet) in a pair of neighboring quantum dots can be carried out using the spin blockade[23] effect. This physical property of Jacobi states will be used later.

Next we discuss the linear TQD model where $J_{12} = J_{23} = J_0$ and $J_{13} = 0$ in Eq. (2). In this case, the three eigenstates[13,14,20] are given by $|L_0\rangle$, $|L_1\rangle$, and $|q_0\rangle$, respectively. The two Jacobi states, $|L_0\rangle$ and $|L_1\rangle$, constitute the levels of a coded qubit in a linear TQD. Similar to the case of the triangular TQD, the coded qubit Hamiltonian in the basis of $\{|L_{0(1)}\rangle\}$ reads

$$H_{\mathrm{lin}}^{\mathrm{qb}} = \tfrac{1}{4}(J_{12} + J_{23})\hat{\sigma}_x + \tfrac{\sqrt{3}}{4}(J_{23} - J_{12})\hat{\sigma}_z. \quad (6)$$

The coded qubit in a linear TQD is equivalent to a spin-1/2 under an effective field in the X-Z plane.

III. GENERATION OF BERRY'S PHASE

So far we have established the equivalence between a coded qubit in a TQD and a model of a spin-1/2 particle under an effective field $\mathbf{R} = (X, Y, Z)$, which is a function of exchange couplings J_{ij}. To generate Berry's phase, we need to adiabatically rotate the effective field $\mathbf{R}$ along a closed loop encircling the diabolical point[1,2,24] in the parameter space of $\mathbf{R}$. For a two-level system under magnetic field, there exists only one diabolical point which lies at the origin of the parameter space.

When the effective field $\mathbf{R}$ is adiabatically varied, the wave function $|\psi(0)\rangle = |n(\mathbf{R}(0))\rangle$ initialized in the nth eigenstate of the Hamiltonian at time 0 evolves as follows:[2]

$$|\psi(t)\rangle = T e^{-(i/\hbar)\int dt' \epsilon_n(\mathbf{R}(t'))} e^{i\gamma_n(t)}\,|n(\mathbf{R}(t))\rangle, \quad (7)$$

where the integral over the nth eigenenergy, $\epsilon_n(\mathbf{R}(t'))/\hbar$, is the accumulated dynamical phase and $\gamma_n(t)$ is the accumulated geometrical phase. We remark that $|n(\mathbf{R}(t))\rangle$ should be chosen to be single-valued and the phase of the eigenstates at different $\mathbf{R}$ should be continuously differentiable with respect to $\mathbf{R}$.

After the system is transported around the closed circuit C in one period T, the system returns to the initial state $|n(\mathbf{R}(0))\rangle$

with a Berry's phase defined by $\phi_n(C) \equiv \gamma_n(T)$. For two-level systems, we use $n = \pm$ to denote the two possible states. The accumulated Berry's phase has an analytical expression[2] in the two-level case, $\phi_\pm(C) = \mp\frac{1}{2}\Omega(C)$, where $\Omega(C)$ is the solid angle subtended by the closed circuit with respect to the origin of the parameter space.

Now we turn to the discussion of generating the Herzberg circuit for a TQD. It is clear that the effective field $X(J_{ij})$ and $Y(J_{ij})$ in Eq. (5) as a function of exchange couplings can be made to form a closed path encircling the origin in the parameter space, if all three exchange interactions J_{ij} can be controlled independently. In experiments, J_{ij} are manipulated through tuning E_i and t_{ij}. The simplest attempt to construct the closed loop in the X-Y plane is to vary the on-site energy of each dot. However, this proposal fails because each exchange interaction J_{ij} depends on the on-site energies of dot i and j through their energy difference ΔE_{ij}. We note that a constraint $\Delta E_{12} + \Delta E_{23} + \Delta E_{31} = 0$ is implicitly imposed on these energy differences. Therefore, we have only two degrees of freedom with the on-site energies. We need to tune at least one tunnel coupling. For instance, the effective field can be rotated on a circle with radius J by tuning E_1, E_3, and t_{13}, while $E_2 = E$, $t_{23} = t_{12} = t$ are being held constant. Furthermore, we select values of E_1, E_3, and t_{13} at each point on the circle such that $J_{13} = \frac{4\eta}{\sqrt{3}}J$ is satisfied at all times with η being an arbitrary constant. Given these conditions, we construct a Herzberg circuit by tuning the following parameters:

$$E_1(\theta) = E + \sqrt{(U-V)^2 - \frac{4(U-V)|t|^2}{\frac{J}{\beta}(\eta - \sin\theta)}}, \tag{8}$$

$$E_3(\theta) = E + \sqrt{(U-V)^2 - \frac{4(U-V)|t|^2}{\frac{J}{2\alpha}\cos\theta + \frac{J}{2\beta}(2\eta - \sin\theta)}}, \tag{9}$$

$$t_{13}(\theta) = \sqrt{\frac{[(U-V)^2 - (E_1 - E_3)^2]\eta J}{4\beta(U-V)}}, \tag{10}$$

where $\alpha = 1/4$, $\beta = \sqrt{3}/4$, and θ is the accumulated angle on the closed circuit. Figures 2(a) and 2(b) present the tuning of the ΔE_{12}, ΔE_{23}, and t_{13} as functions of θ, and Fig. 2(c) shows the response of J_{ij} due to the changes in the Hubbard parameters. Figure 2(d) shows the Herzberg circuit with radius J in the parameter space $\mathbf{R}$ for the effective spin-1/2 model.

The two lowest states in the $S_y = -1/2$ subspace of a TQD can be mapped onto the coded qubit model, Eq. (5), only when on-site Coulomb repulsion is the dominant energy scale. However, we note that the variations in ΔE_{13} and ΔE_{23} can reach $0.58\,U$ at certain points on the circuit, as shown in Fig. 2. The validity of the Heisenberg model becomes questionable over the course of transporting the system around the circuit in Fig. 2. Thus, we expect that a more realistic circuit, which minimizes the variations of all ΔE_{ij}, would require tuning

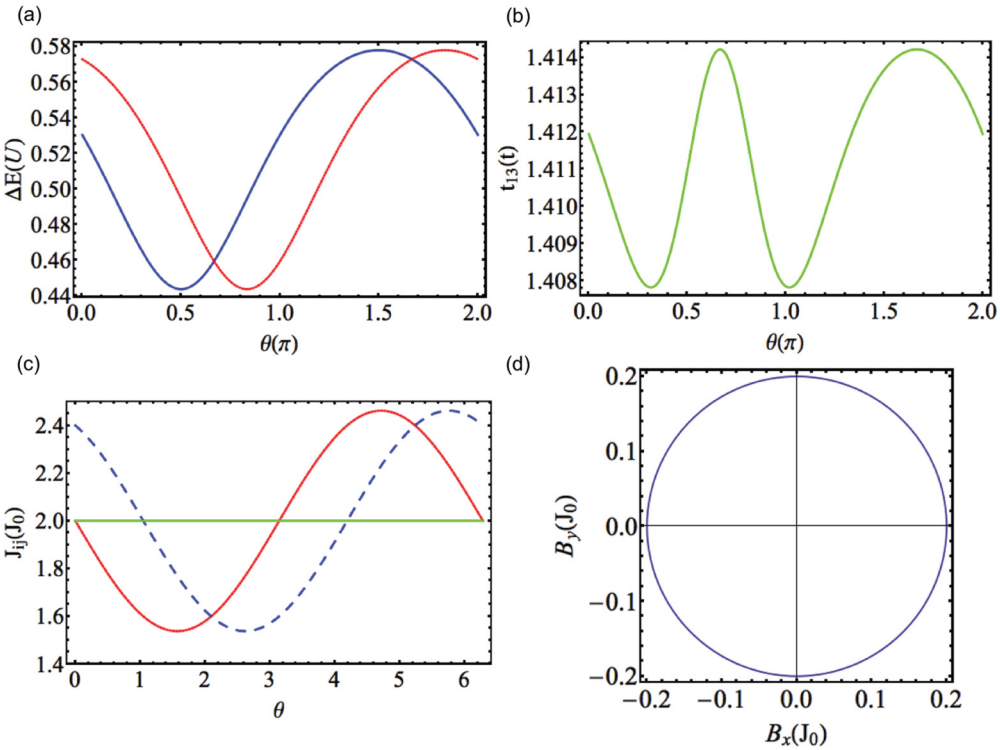

FIG. 2. (Color online) (a) Variations of ΔE_{12} (blue curve) and ΔE_{23} (red curve) over one round on the closed circuit. Note that the variation is comparable to U, the largest energy scale of the Hubbard model. (b) Variation of t_{13} over one round on the closed circuit. (c) The values of J_{ij}, computed with Eq. (3), over one round on the closed circuit. J_{12} is red, J_{23} is blue, and J_{13} is green. This circuit is generated under the constraint that J_{13} is constant. (d) Parametric plot of the closed circuit itself in the parameter space $\mathbf{R}$ for the coded qubit (effective two-level system). The x and y components of the circle are related to the J_{ij} via the real and imaginary components of the off-diagonal matrix element in Eq. (5).

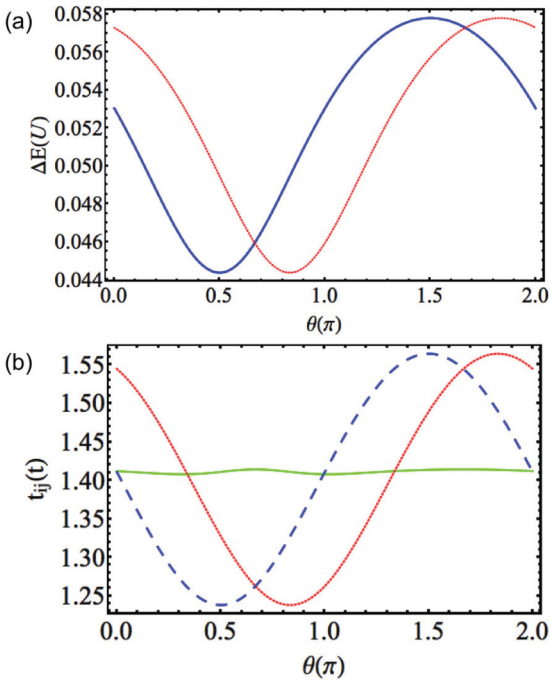

FIG. 3. (Color online) (a) Variations of ΔE_{12} (blue) and ΔE_{23} (red) over one round on the closed circuit. The variations of ΔE_{ij} are significantly suppressed when compared to Fig. 2(a). This is because we vary all t_{ij}. (b) Variation of t_{ij} over one round on the closed circuit. t_{12} is blue, t_{23} is red, and t_{13} is green. The values of t_{ij} are chosen specifically to reproduce the same J_{ij} in Fig. 2(c) and reduce the variations of ΔE_i.

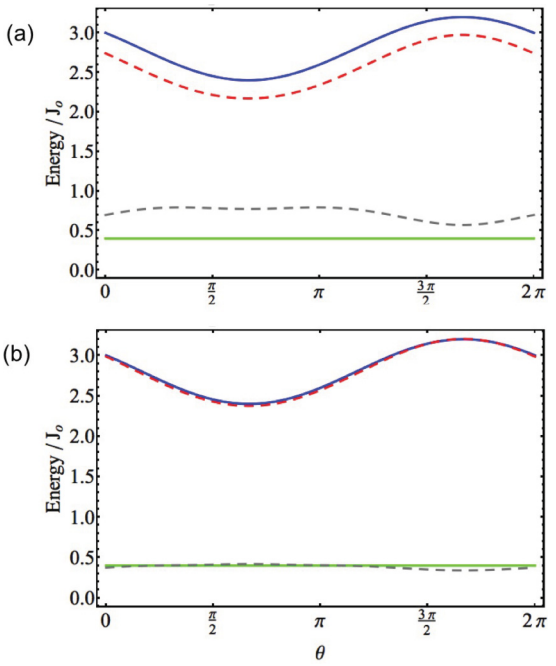

FIG. 4. (Color online) (a) The energy gap $\epsilon_2 - \epsilon_1$ (top figure) as well as $\epsilon_1 - \epsilon_0$ (bottom figure) in both Hubbard (dotted curve) and Heisenberg (solid curve) model for the circuit presented in Fig. 2. ϵ_i is the ith eigenenergy of the system. (b) The same energy gaps in both Hubbard (dotted) and Heisenberg (solid) model for the circuit presented in Fig. 3. In both (a) and (b), the green, solid curve which represents the energy gap between the two coded qubit levels is a constant over the closed circuit. This is because we transport the coded qubit on a constant energy surface as implied by the parametric plot of $\{B_x, B_y\}$ for the coded qubit (effective two-level system) in Fig. 2(d).

more than E_1, E_3, and t_{13}. For instance, Figs. 3(a) and 3(b) present another circuit, which involves tuning all E_i and t_{ij} but E_2 in order to produce identical J_{ij} as shown in Fig. 2(c) and also the same circuit as shown in Fig. 2(d). By moderately tuning t_{12} and t_{23}, we observe that the need to tune ΔE_{ij} is significantly reduced as shown in Fig. 3(a). Figures 4(a) and 4(b) compare the energy gap between the lowest three levels in the Hubbard model and the Heisenberg model in the $S_y = -1/2$ subspace for the circuits presented in Figs. 2 and 3, respectively. As shown, the second circuit, which tunes all t_{ij}, provides a better agreement between results of the Hubbard and Heisenberg models. To manipulate the dynamical phase of the coded qubit, a fast tuning of on-site energies is preferred. However, in the case of the adiabatic accumulation of geometrical phases, gating operations should be done slowly and the tuning of the tunnel couplings might be more favorable.

Figure 5 shows the numerical computation of accumulated geometrical phase for the coded qubit along the Herzberg circuit presented in Fig. 2. After one round on the circuit, the state accumulates a geometric phase of π. To generate the figure, we simulate the time evolution of the coded qubit, which was initialized in the ground state at time $t = 0$, by tuning the on-site energies and tunnel coupling according to Eqs. (8)–(10). At time step θ which denotes the fraction of the Herzberg circuit, we diagonalize the parametrized Heisenberg Hamiltonian and express the wave function $|\psi(\theta)\rangle = \sum_{n=-1,0,1} c_n(\theta)|n(R_\theta)\rangle$. To update the wave function to $|\psi(\theta + \Delta\theta)\rangle$, we add a dynamical phase $e^{-i\omega_n(\theta)\Delta\theta}$ to $c_n(\theta)$ with $\omega_n(\theta)$ being proportional to the nth eigenenergies. In order to extract the geometrical phase, we follow Eq. (7) and evaluate the following inner product $e^{i\gamma_n(\theta)} = e^{i\omega_n\theta}\langle n(R_\theta)\,|\,\psi(\theta)\rangle$, where $\omega_n(\theta)$ is a constant along the Herzberg circuit (a circle in the parameter space).

Having demonstrated explicitly the generation of Berry's phase in a triangular triple quantum dot, we now focus on the coded qubit in a linear TQD. We note that the diagonal

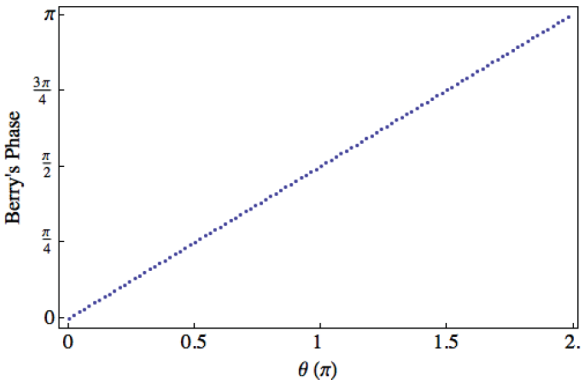

FIG. 5. (Color online) Accumulation of Berry's phase by the coded qubit level, $|q_+\rangle$. At the end of the Herzberg circuit, $\theta = 2\pi$, the accumulated phase is π, in agreement with theory.

element H_{11} of the Hamiltonian, Eq. (6), is always positive because all $J_{ij} > 0$. The effective magnetic field component in the Z direction is always positive, and no closed loop can be made to encircle the origin of the parameter space. Hence we conclude that it is not possible to generate Herzberg circuit and Berry's phase with a coded qubit in a linear TQD.

IV. DETECTION OF BERRY'S PHASE

Let us now turn to a possible experimental observation of Berry's phase using quantum interference in a triangular TQD. For the chirality-based coded qubit, the effective field $\mathbf{R}$ is restricted to the X-Y plane. The solid angle subtended by any closed circuit in the X-Y plane is either 0 or π, depending on whether the closed circuit encircles the origin or not. The limited range of Berry's phase prevents an easy way to extract the phase through quantum interference. Therefore, it is essential to have a modified Herzberg circuit that is lifted above the X-Y plane, so the solid angle subtended by the circuit is given by $\Omega = 2\pi(1 - \cos\theta)$, where $\cos\theta = Z/(X^2 + Y^2 + Z^2)^{1/2}$ is the direction cosine on the Bloch sphere. To generate R with a Z component, we need to apply a magnetic field B_z perpendicular to the triangular TQD. The real field B_z turns on the chiral term χ_{ijk} in Eq. (2). Since the chiral states are eigenstates of the chirality operator, the chirality term acts as a $\hat{\sigma}_z$ operation in the coded qubit subspace. The coefficient, χ_{ijk}, attached to the chirality operator is $\approx |t|^3/U^2$. If we take $t = -0.05$ and $U = 2.0$, the values used to generate Fig. 3, then χ_{ijk} is about two to three orders of magnitude smaller than J_{ij}. It is important to realize that χ_{ijk}, derived from third-order perturbation theory, also depends on the TQD parameters such as t_{ij}, and differences of on-site energies through terms like $1/[(U - V + \Delta E_{ij})(U - V + \Delta E_{ki})]$. Therefore, as the system is adiabatically transported on a closed circuit by varying the gate voltage, the magnitude of this effective Z field will oscillate in its magnitude. An estimated change of the Z field over the course of one complete circuit is two to three orders of magnitude smaller than that of the X and Y fields.

Following Ref. 8, we now describe a possible procedure to experimentally detect Berry's phase in a triangular TQD. First, we prepare the coded qubit in a linear superposition of the form $\frac{1}{\sqrt{2}}|q_+\rangle + \frac{1}{\sqrt{2}}|q_-\rangle$ by having an effective field $\mathbf{R}$ along the Y direction. Next, we apply a B_z field to generate $\mathbf{R}$ with a Z component. Then we tune the parameters E_{ij} and t_{ij} as shown in Fig. 3 to accumulate the geometrical phase over one cyclic evolution on the circuit lying above the X-Y plane. After one cyclic evolution with a period T, the states $|q_\pm\rangle$ acquire a phase $\pm\delta(T) + \phi_\pm(C)$, where $\delta(T)$ is the dynamical phase for state $|q_+\rangle$. We then apply a spin-echo[7,8,12] like procedure to eliminate the dynamical phases. We first perform a NOT operation ($\hat{\sigma}_x$ operation) on the coded qubit to flip the two chiral states, and this step can be achieved by rapidly tuning[25] only E_{ij} to minimize any additional changes to the states. So the overall phase factor associated with $|q_\pm\rangle$ is $\mp\delta(T) + \phi_\mp(C)$. Then we transport the system around the same circuit in the opposite direction. According to Eq. (7), the dynamical phase only depends on the eigenenergies along the circuit. Since it is the same circuit, the state acquires the same dynamical phase as before, but the sign of Berry's phase depends on the direction of traversal on the circuit. Therefore, the states $|q_\pm\rangle$ each acquire an additional phase factor $\pm\delta(T) - \phi_\pm(C)$ during the second round on the circuit. Finally, we remove the B_z field to return the system into the X-Y plane. As discussed in Ref. 8, the accumulated dynamical and geometrical phases during the processes of applying and removing B_z actually cancel each other exactly. Therefore, we can combine the phase factors accumulated over the two complete rounds of the closed circuit to get the final state, $|\psi_f\rangle = \frac{1}{\sqrt{2}}e^{-i2\phi_+}|q_+\rangle + \frac{1}{\sqrt{2}}e^{i2\phi_+}|q_-\rangle$, where the dynamical phases add destructively and only geometrical phase is left.

The final task is to perform quantum interferometry to extract Berry's phase from the system. We note that the Jacobi states can be written as a linear combination of the two chiral states,

$$\begin{aligned} |L_0\rangle &= (-ie^{i2\pi/3}/\sqrt{2})|q_+\rangle + (ie^{-i2\pi/3}/\sqrt{2})|q_-\rangle, \\ |L_1\rangle &= (-e^{i2\pi/3}/\sqrt{2})|q_+\rangle - (e^{-i2\pi/3}/\sqrt{2})|q_-\rangle. \end{aligned} \tag{11}$$

This implies that, for instance, the probability amplitude of measuring $|L_{0,1}\rangle$ state with respect to $|\psi_f\rangle$ is given by

$$\begin{aligned} \langle L_0|\psi_f\rangle &= \sin\left(2\phi_+ + \frac{2\pi}{3}\right), \\ \langle L_1|\psi_f\rangle &= -\cos\left(2\phi_+ + \frac{2\pi}{3}\right). \end{aligned} \tag{12}$$

It is clear that the result of projective measurements in the Jacobi basis depends on Berry's phase $\phi_+(C)$.

Experiments[23,25,26] have already demonstrated that the joint spin states between two neighboring dots can be measured by the spin to charge conversion. If the charge detection shows that charge configuration (1,1,1) converts to charge configuration (2,1,0), then we have a $|L_0\rangle$ state in the triangular TQD. Repeating the procedures of accumulating Berry's phase with different ratios of $Z^2/(X^2 + Y^2 + Z^2)$, one can extract Berry's phase following Eq. (12).

Once the modified Herzberg circuit is lifted from the X-Y plane, the Berry's phase depends on the geometry of the circuit. Major sources of decoherences include fluctuating charges[27] and nuclear spins.[28] In the simplest approximation, the effects of these two types of environment on the coded qubit can be approximated with a spin-1/2 model in the presence of a random fluctuating field $\mathbf{R}_{\text{rand}}$. Such a model was already studied in Ref. 29, which showed that Berry's phase is more robust than the dynamical phase.

V. CONCLUSION

In summary, we presented a theoretical proposal for the Herzberg circuit and controlled accumulation of Berry's phase in a qubit encoded in the two degenerate chirality states of a three-spin complex with total spin $S = 1/2$ in a triangular triple quantum dot molecule with one electron spin each. Using a Hubbard and Heisenberg model the Herzberg circuit encircling the degeneracy point is realized by adiabatically tuning the successive on-site energies of quantum dots and tunnel couplings across pairs of neighboring dots. It is explicitly shown that encircling the degeneracy point leads to the accumulation of the geometrical Berry's phase. We show that only the triangular, not the linear, quantum dot molecule

allows for the generation of Berry's phase and we discuss a protocol to detect this geometrical phase in interference experiments relying on spin to charge conversion in spin blockade and/or charge sensing spectroscopy.

ACKNOWLEDGMENT

The authors thank CIFAR, NSERC, QUANTUMWORKS, and OGS for financial support.

[1]G. Herzberg and H. Longuet-Higgins, Discuss. Faraday Soc. **35**, 77 (1963).
[2]M. Berry, Proc. R. Soc. London A **392**, 45 (1984).
[3]F. Wilczek and A. Shapere, *Geometric Phases in Physics* (World Scientific, 1988).
[4]A. C. M. Carollo and V. Vedral, in *Holonomic Quantum Computation*, Lectures on Quantum Information, edited by D. Bruß and G. Leuchs (Wiley-VCH Verlag GmbH, Weinheim, Germany, 2008), pp. 381–387.
[5]J. Pachos, P. Zanardi, and M. Rasetti, Phys. Rev. A **61**, 010305 (1999).
[6]T. Bitter and D. Dubbers, Phys. Rev. Lett. **59**, 251 (1987).
[7]J. A. Jones, V. Vedral, A. Ekert, and G. Castagnoli, Nature (London) **403**, 1 (2000).
[8]P. J. Leek, J. M. Fink, A. Blais, R. Bianchetti, M. Göppl, J. M. Gambetta, D. I. Schuster, L. Frunzio, R. J. Schoelkopf, and A. Wallraff, Science **318**, 1889 (2007).
[9]M. Möttönen, J. J. Vartiainen, and J. P. Pekola, Phys. Rev. Lett. **100**, 177201 (2008).
[10]M. Aunola and J. J. Toppari, Phys. Rev. B **68**, 020502(R) (2003).
[11]J. P. Pekola, J. J. Toppari, M. Aunola, M. T. Savolainen, and D. V. Averin, Phys. Rev. B **60**, R9931 (1999).
[12]G. Falci, R. Fazio, G. M. Palma, J. Siewert, and V. Vedral, Nature (London) **407**, 355 (2000).
[13]P. Hawrylak and M. Korkusinski, Solid State Commun. **136**, 508 (2005).
[14]C.-Y. Hsieh and P. Hawrylak, Phys. Rev. B **82**, 205311 (2010).
[15]D. DiVincenzo, D. Bacon, J. Kempe, and G. Burkard, Nature (London) **408**, 339 (2000).
[16]L. Gaudreau, S. A. Studenikin, A. S. Sachrajda, P. Zawadzki, A. Kam, J. Lapointe, M. Korkusinski, and P. Hawrylak, Phys. Rev. Lett. **97**, 036807 (2006).
[17]L. Gaudreau, A. Kam, G. Granger, S. A. Studenikin, P. Zawadzki, and A. S. Sachrajda, Appl. Phys. Lett. **95**, 193101 (2009).
[18]G. Granger, L. Gaudreau, A. Kam, M. Pioro-Ladrière, S. A. Studenikin, Z. R. Wasilewski, P. Zawadzki, and A. S. Sachrajda, Phys. Rev. B **82**, 075304 (2010).
[19]E. A. Laird, J. M. Taylor, D. P. DiVincenzo, C. M. Marcus, M. P. Hanson, and A. C. Gossard, Phys. Rev. B **82**, 075403 (2010).
[20]M. Korkusinski, I. P. Gimenez, P. Hawrylak, L. Gaudreau, S. A. Studenikin, and A. S. Sachrajda, Phys. Rev. B **75**, 115301 (2007).
[21]V. W. Scarola, K. Park, and S. Das Sarma, Phys. Rev. Lett. **93**, 120503 (2004).
[22]V. W. Scarola and S. Das Sarma, Phys. Rev. A **71**, 032340 (2005).
[23]A. C. Johnson, J. R. Petta, C. M. Marcus, M. P. Hanson, and A. C. Gossard, Phys. Rev. B **72**, 165308 (2005).
[24]M. Berry and M. Wilkinson, Proc. R. Soc. A **392**, 15 (1984).
[25]J. Petta, A. Johnson, J. Taylor, E. Laird, A. Yacoby, M. D. Lukin, C. M. Marcus, and M. P. Hanson, Science **309**, 2180 (2005).
[26]F. Koppens, C. Buizert, K. Tielrooij, and I. Vink, Nature (London) **442**, 766 (2006).
[27]I. P. Gimenez, C. Y. Hsieh, M. Korkusinski, and P. Hawrylak, Phys. Rev. B **79**, 205311 (2009).
[28]I. A. Merkulov, A. L. Efros, and M. Rosen, Phys. Rev. B **65**, 205309 (2002).
[29]G. De Chiara and G. M. Palma, Phys. Rev. Lett. **91**, 090404 (2003).